Generation and growth rates of nonlinear distortions in a traveling wave tube

John G. Wöhlbier, Ian Dobson, and John H. Booske
Department of Electrical and Computer Engineering, University of Wisconsin, Madison, Wisconsin 53706
(Received 9 April 2002; published 22 November 2002)

The structure of a steady state multifrequency model of a traveling wave tube amplifier is exploited to describe the generation of intermodulation frequencies and calculate their growth rates. The model describes the evolution of Fourier coefficients of circuit and electron beam quantities and has the form of differential equations with quadratic nonlinearities. Intermodulation frequencies are sequentially generated by the quadratic nonlinearities in a series solution of the differential equations. A formula for maximum intermodulation growth rates is derived and compared to simulation results.

DOI: 10.1103/PhysRevE.66.056504 PACS number(s): 52.59.Rz, 84.40.Fe, 84.47.+w, 52.35.Mw

Traveling wave tubes (TWTs) continue to find widespread application as amplifiers due to their inherently wide bandwidths and their high frequency, high power operating points. Due to the advent of very accurate models [1], TWT bandwidths continue to increase and bandwidths as large as three octaves are being approached [2]. Understanding and quantifying the nonlinear distortions in wide bandwidth TWTs remains a challenge.

The nonlinear distortion in TWTs is ''intermodulation distortion.'' For steady-state input signals with multifrequency content, an intermodulation product of order K for frequencies $f_1, f_2, \ldots, f_P$ is of the form $r_1 f_1 + r_2 f_2 + \ldots + r_P f_P$, where r_j are integers (possibly zero) and $K = |r_1| + |r_2| + \ldots + |r_P|$. This structure also includes harmonic frequencies when all but one of the r_j's are zero.

The most basic piece of information about the behavior of an intermodulation product (IMP) is its exponential growth rate prior to saturation. In this paper, we study IMP growth rates in the S-MUSE TWT model [3], which has the form of ordinary differential equations with quadratic nonlinearities. We show how IMP frequencies are sequentially generated by the quadratic nonlinearities. We give a series solution of the nonlinear differential equations and take advantage of the generating structure to compute maximum IMP growth rates. This approach provides growth rate estimates and insight into the generation of the IMPs.

S-MUSE is a nonlinear, multifrequency, steady-state TWT model. It is a simplification of the more complete MUSE model also derived in Ref. [3]. The electron beam is modeled using Eulerian equations, so S-MUSE does not predict electron overtaking. However, S-MUSE captures much of the important nonlinear physics that occurs prior to electron overtaking, and compares favorably to large signal codes prior to saturation [3].

The S-MUSE model consists of nonlinear ordinary differential equations for the Fourier coefficients of circuit voltage $\tilde{V}_\ell$, circuit current $\tilde{I}_\ell$, space charge electric field $\tilde{E}_\ell$, electron beam velocity $\tilde{v}_\ell$, and electron beam charge density $\tilde{\rho}_\ell$ as functions of axial position z. All frequencies are integer multiples of a fundamental frequency ω_0, i.e., $f = f_\ell \omega_0$. The subscript ℓ indexes the frequencies f_ℓ contained in the set Ω which will be discussed shortly. The frequency dependent parameters $\tilde{K}_\ell, \tilde{v}_{\mathrm{ph}\ell}$, and $\tilde{R}_\ell$ are circuit interaction impedance, cold circuit phase velocity, and space charge reduction factor, respectively [4]. The electron beam cross sectional area is A and the dc electron beam velocity is u_0. The S-MUSE model [3] is

$$\frac{d\tilde{V}_\ell}{dz} = -\frac{if_\ell\omega_0}{u_0}\tilde{V}_\ell - \frac{if_\ell\omega_0\tilde{K}_\ell}{\tilde{v}_{\mathrm{ph}\ell}}\tilde{I}_\ell, \tag{1}$$

$$\frac{d\tilde{I}_\ell}{dz} = -\frac{if_\ell\omega_0}{\tilde{K}_\ell\tilde{v}_{\mathrm{ph}\ell}}\tilde{V}_\ell - \frac{if_\ell\omega_0}{u_0}\tilde{I}_\ell + if_\ell\omega_0 A\tilde{\rho}_\ell, \tag{2}$$

$$\frac{d\tilde{E}_\ell}{dz} = -\frac{if_\ell\omega_0}{u_0}\tilde{E}_\ell + \frac{\tilde{\rho}_\ell}{\epsilon_0}, \tag{3}$$

$$\frac{d\tilde{v}_\ell}{dz} = \frac{if_\ell\omega_0 e\tilde{K}_\ell}{m_e u_0\tilde{v}_{\mathrm{ph}\ell}}\tilde{I}_\ell + \frac{e}{m_e u_0}\tilde{R}_\ell\tilde{E}_\ell - \frac{1}{u_0^2}\sum_{\substack{m,n\\ f_m+f_n=f_\ell}} if_n\omega_0\tilde{v}_m\tilde{v}_n, \tag{4}$$

$$\begin{aligned}\frac{d\tilde{\rho}_\ell}{dz} = &-\frac{if_\ell\omega_0 e\rho_0\tilde{K}_\ell}{m_e u_0^2\tilde{v}_{\mathrm{ph}\ell}}\tilde{I}_\ell - \frac{e\rho_0}{m_e u_0^2}\tilde{R}_\ell\tilde{E}_\ell - \frac{if_\ell\omega_0\rho_0\tilde{v}_\ell}{u_0^2}\\ &-\frac{e}{m_e u_0^2}\sum_{\substack{m,n\\ f_m+f_n=f_\ell}}\frac{if_m\omega_0\tilde{K}_m}{\tilde{v}_{\mathrm{ph}m}}\tilde{I}_m\tilde{\rho}_n\\ &-\frac{e}{m_e u_0^2}\sum_{\substack{m,n\\ f_m+f_n=f_\ell}}\tilde{R}_m\tilde{E}_m\tilde{\rho}_n + \frac{\rho_0}{u_0^3}\sum_{\substack{m,n\\ f_m+f_n=f_\ell}} if_n\omega_0\tilde{v}_m\tilde{v}_n\\ &-\frac{if_\ell\omega_0}{u_0^2}\sum_{\substack{m,n\\ f_m+f_n=f_\ell}}\tilde{v}_m\tilde{\rho}_n,\end{aligned} \tag{5}$$

where $-M \leq \ell \leq M, \ell \neq 0$. The summations in Eqs. (4) and (5) are over integers m,n such that $f_m + f_n = f_\ell$.

Equations (1)–(5) may be written in vector form as the sum of a linear and quadratic term

$$\dot{\mathbf{x}}_\ell = \mathbf{A}_\ell \mathbf{x}_\ell + \sum_{\substack{m,n \\ f_m + f_n = f_\ell}} \mathbf{H}_{\ell mn}(\mathbf{x}_m, \mathbf{x}_n), \tag{6}$$

where $\mathbf{x}_\ell = [\tilde{V}_\ell \tilde{I}_\ell \tilde{E}_\ell \tilde{v}_\ell \tilde{\rho}_\ell]^{\mathrm{T}}$. In Eq. (6), the product $\mathbf{A}_\ell \mathbf{x}_\ell$ contains the linear terms in Eqs. (1)–(5), and the term $\Sigma \mathbf{H}_{\ell mn}(\mathbf{x}_m, \mathbf{x}_n)$ represents the quadratic terms in Eqs. (4)–(5). (The entries of $\mathbf{A}_\ell$ and $\mathbf{H}_{\ell mn}$ are described in detail in Appendix II of Ref. [3].) The dispersion properties of the TWT are contained in $\mathbf{A}_\ell$ and $\mathbf{H}_{\ell mn}$. We can write the equations for all frequencies together as

$$\dot{\mathbf{x}} = \mathbf{A}\mathbf{x} + \mathbf{H}(\mathbf{x}, \mathbf{x}), \tag{7}$$

$$\mathbf{x}(0) = \mathbf{w}, \tag{8}$$

where $\mathbf{x} = [\mathbf{x}_{-M} \cdots \mathbf{x}_{-1} \mathbf{x}_1 \cdots \mathbf{x}_M]^{\mathrm{T}}$. The vector $\mathbf{w}$ contains the initial data of the drive frequencies.

We solve [8] the nonlinear differential equation (7) with the series

$$\mathbf{x} = \sum_{\alpha=1}^{\infty} \mathbf{x}^{(\alpha)}, \tag{9}$$

with superscript (α) an index, not an exponent. The components of the series satisfy the equations

$$\dot{\mathbf{x}}^{(1)} = \mathbf{A}\mathbf{x}^{(1)}, \quad \mathbf{x}^{(1)}(0) = \mathbf{w}, \tag{10}$$

$$\dot{\mathbf{x}}^{(\alpha)} = \mathbf{A}\mathbf{x}^{(\alpha)} + \sum_{\beta=1}^{\alpha-1} \mathbf{H}(\mathbf{x}^{(\beta)}, \mathbf{x}^{(\alpha-\beta)}), \tag{11}$$

$$\mathbf{x}^{(\alpha)}(0) = \mathbf{0}, \quad \alpha = 2,3,4, \ldots .$$

One can show that the series solution (9) converges geometrically for $z \leqslant L$ if $|\mathbf{w}| \|\mathbf{H}\| (e^{\sigma L} - 1)/\sigma < 1$, where σ is the largest of the real parts of the eigenvalues of $\mathbf{A}$. ($|\cdot|$ and $\|\cdot\|$ are vector and induced l^1 norms in modal coordinates.) The ℓth component of Eq. (11) is

$$\dot{\mathbf{x}}_\ell^{(\alpha)} = \mathbf{A}_\ell \mathbf{x}_\ell^{(\alpha)} + \sum_{\beta=1}^{\alpha-1} \sum_{\substack{m,n \\ f_m + f_n = f_\ell}} \mathbf{H}_{\ell mn}(\mathbf{x}_m^{(\beta)}, \mathbf{x}_n^{(\alpha-\beta)}), \quad \alpha = 2,3,4, \ldots . \tag{12}$$

The quadratic term in Eq. (12) dictates how frequency components of $\mathbf{x}^{(1)}, \mathbf{x}^{(2)}, \ldots, \mathbf{x}^{(\alpha-1)}$ combine to produce frequency components of $\mathbf{x}^{(\alpha)}$. In particular, the solutions for the drive frequencies in $\mathbf{x}^{(1)}$ produce components in $\mathbf{x}^{(2)}$ for frequencies that are all possible additions of pairs of drive frequencies (and the negatives of the drive frequencies). Then, components of $\mathbf{x}^{(1)}$ and $\mathbf{x}^{(2)}$ produce components in $\mathbf{x}^{(3)}$ for frequencies which are all possible additions of pairs of frequencies from $\mathbf{x}^{(1)}$ and $\mathbf{x}^{(2)}$. Similarly, components of $\mathbf{x}^{(1)}$ and $\mathbf{x}^{(3)}$ and components of $\mathbf{x}^{(2)}$ and $\mathbf{x}^{(2)}$ combine to produce components of $\mathbf{x}^{(4)}$ and so on.

To keep track of the frequencies generated in this process we construct sets $\Omega^{(\alpha)}$ that contain the frequencies generated in the term $\mathbf{x}^{(\alpha)}$. For example, if f_a and f_b are drive frequencies, then we define $\Omega^{(1)}$ to contain the drive frequencies and the negative drive frequencies:

$$\Omega^{(1)} = \{-f_b, -f_a, f_a, f_b\}. \tag{13}$$

From Eq. (12), the frequencies produced in the second series term are

$$\Omega^{(2)} = \{-2f_b, -f_a - f_b, -2f_a, f_a - f_b, -f_a + f_b, 2f_a, f_a + f_b, 2f_b\}. \tag{14}$$

Similarly, frequencies in $\mathbf{x}^{(3)}$ are all possible additions of frequency pairs including one from $\Omega^{(1)}$ and one from $\Omega^{(2)}$:

$$\Omega^{(3)} = \{-3f_b, -f_a - 2f_b, -2f_a - f_b, -3f_a, f_a - 2f_b, -f_b, -f_a, -2f_a + f_b, 2f_a - f_b, f_a, f_b, -f_a + 2f_b, 3f_a, 2f_a + f_b, f_a + 2f_b, 3f_b\}. \tag{15}$$

Notice that $\Omega^{(3)}$ contains third harmonics and 3IMs, but also contains the drive frequencies.

In general, $\Omega^{(1)}$ contains the positive and negative drive frequencies, and we define $\Omega^{(\alpha)}, \alpha = 2,3,4, \ldots$ by

$$\Omega^{(\alpha)} = \{f + g \,|\, f \in \Omega^{(\beta)}, \; g \in \Omega^{(\alpha-\beta)}, \; 1 \leqslant \beta \leqslant \alpha - 1, \; f + g \neq 0\}. \tag{16}$$

In applications, we truncate the frequency generation process described above. Since the highest order of IMP in $\Omega^{(\alpha)}$ is equal to α, we let S to be the highest order IMP of interest and then define Ω to be all of the frequencies in $\Omega^{(1)}, \ldots, \Omega^{(S)}$. Order Ω as

$$\Omega = \{f_{-M} f_{-M+1} \cdots f_{-1} f_1 \cdots f_{M-1} f_M\}, \tag{17}$$

where $f_\ell > f_m$ if $\ell > m$ and $f_{-\ell} = -f_\ell$. The indices of Ω are then used to index $\mathbf{x}$.

Recall that $\mathbf{x}_\ell^{(\alpha)}$ is term α in the series solution for frequency f_ℓ. By solving the linear system (10) and then successively solving the forced linear systems (11), it can be shown that $\mathbf{x}_\ell^{(\alpha)}$ is a sum of exponentials of the form

$$\mathbf{x}_\ell^{(\alpha)}(z) = \sum_{p=1}^{P} \mathbf{a}_\ell^{(\alpha)[p]} \exp(\mu_\ell^{(\alpha)[p]} + i\sigma_\ell^{(\alpha)[p]}) z, \tag{18}$$

where $\mathbf{a}_\ell^{(\alpha)[p]}$ is a complex vector and $\mu_\ell^{(\alpha)[p]}$, $\sigma_\ell^{(\alpha)[p]}$ are real. The assumptions underlying Eq. (18) are discussed in Ref. [9]. Sums, such as Eq. (18), are ordered so that $\mu_\ell^{(\alpha)[1]}$ is the maximum of $\mu_\ell^{(\alpha)[1]}, \mu_\ell^{(\alpha)[2]}, \ldots, \mu_\ell^{(\alpha)[P]}$. Since $\mu_\ell^{(\alpha)[1]}$ is the largest real part of the exponents in $\mathbf{x}_\ell^{(\alpha)}$, we call $\mu_\ell^{(\alpha)[1]}$ the *maximum growth rate* of term α in the series solution for frequency f_ℓ.

Using Eq. (18) and the standard solution of the forced linear system (12) [5], a recursive formula for the growth rate $\mu_\ell^{(\alpha)[1]}$ in terms of $\mu_\ell^{(1)[1]}, \mu_\ell^{(2)[1]}, \ldots, \mu_\ell^{(\alpha-1)[1]}$ is

TABLE I. Growth rates for two drive frequencies and nonlinear products up to order five for the bandwidth of 0.8–9.0 GHz. Results for input powers of $-30\,\mathrm{dB_{sat}}$, $-10\,\mathrm{dB_{sat}}$, and $0\,\mathrm{dB_{sat}}$ are given. μ_{Chr} is growth rate fit to Christine 1D power versus axial distance data at at an axial position in the "small-signal" regime, i.e., after the power curves have reached their asymptotic exponential growth state, but prior to saturation of any of the power curves (see Fig. 1). The percent difference columns compare μ_{Chr} to formula (20) using percent difference $=|\mu_{\mathrm{Chr}}-\text{Eq. (20)}|/\mu_{\mathrm{Chr}}$.

		$-30\,\mathrm{dB_{sat}}$		$-10\,\mathrm{dB_{sat}}$		$0\,\mathrm{dB_{sat}}$	
Order	f (GHz)	μ_{Chr}	Percent difference	μ_{Chr}	Percent difference	μ_{Chr}	Percent difference
1	$f_a=3.0$	0.744		0.764		0.770	
	$f_b=4.1$	0.696		0.728		0.733	
2	f_b-f_a	1.443	0.30	1.514	1.44	1.543	2.53
	$2f_a$	1.487	0.03	1.515	0.83	1.555	0.89
	f_a+f_b	1.438	0.07	1.443	3.37	1.457	3.23
	$2f_b$	1.387	0.27	1.361	6.99	1.338	9.62
3	$2f_a-f_b$	2.185	0.10	2.239	0.75	2.326	2.21
	$2f_b-f_a$	2.135	0.01	2.170	2.29	2.225	0.57
	$3f_a$	2.227	0.15	2.239	2.38	2.249	2.78
4	$2f_b-2f_a$	2.885	0.24	2.930	1.86	3.041	1.10
	$3f_a-f_b$	2.923	0.09	2.966	1.80	3.037	0.26
5	$3f_a-2f_b$	3.625	0.09	3.678	1.91	3.864	2.22
	$3f_b-2f_a$	3.583	0.27	3.664	1.30	3.833	2.39
	$4f_a-f_b$	3.665	0.12	3.724	1.61	3.807	0.22

$$\mu_\ell^{(\alpha)[1]}=\max_{\substack{m,n,\beta\\ f_m+f_n=f_\ell\\ 1\le\beta\le\alpha-1}}\{\mu_m^{(\beta)[1]}+\mu_n^{(\alpha-\beta)[1]},\nu_\ell^{[1]}\} \tag{19}$$

where $\nu_\ell^{[1]}$ is the largest of the real parts of the eigenvalues of $\mathbf{A}_\ell$. $\nu_\ell^{[1]}$ is the *linear growth rate* for frequency f_ℓ obtained from $\dot{\mathbf{x}}_\ell^{(\alpha)}=\mathbf{A}_\ell\mathbf{x}_\ell^{(\alpha)}$, which is the linear part of Eq. (12). $\mu_m^{(\beta)[1]}+\mu_n^{(\alpha-\beta)[1]}$ is the largest real part of the exponents in the quadratic term of Eq. (12) formed by the product of $\mathbf{x}_\ell^{(\beta)}$ and $\mathbf{x}_\ell^{(\alpha-\beta)}$. (We are using the standard fact that a linear system solution is the sum of exponentials involving the natural frequencies of the system and the frequencies of the exponential forcing.)

To summarize, $\mathbf{x}_\ell^{(\alpha)}$ is a solution of the linear system (12) forced by products of smaller terms, which are themselves sums of exponentials. Therefore $\mathbf{x}_\ell^{(\alpha)}$ contains both exponentials from the linear portion of Eq. (12) and exponentials from the products of the smaller terms. Formula (19) states that the maximum growth rate $\mu_\ell^{(\alpha)[1]}$ of $\mathbf{x}_\ell^{(\alpha)}$ is the maximum real part of the exponents of all of the exponentials.

Next we present examples illustrating the IMP generation and the application of formula (19). The TWT dispersion and beam parameters are based on a slightly modified experimental Wisconsin Northrup Grumman (XWING) wideband TWT [6]. Formula (19) is checked against growth rates obtained from Christine 1D [7].

First we consider two drive frequencies f_a and f_b separated by 1.1 GHz. In the bandwidth between 0.8 and 9.0 GHz, twelve IMPs of order five and lower are generated; all of the IMPs are of the form mf_a-nf_b. For the IMP frequencies and dispersion parameters in this example, Eq. (19) predicts the growth rate as m times the growth rate of f_a plus n times the growth rate of f_b:

$$m\mu_a^{(1)[1]}+n\mu_b^{(1)[1]}. \tag{20}$$

That is, for the frequencies that make up these IMPs, the linear growth rates $\nu_\ell^{[1]}$ in Eq. (19) are always less than the forcing growth rates $\mu_m^{(\beta)[1]}+\mu_n^{(\alpha-\beta)[1]}$. For a large class of TWT dispersion parameters, Eq. (20) is the correct formula for the maximum growth rate of IMPs of the form mf_a-nf_b.

In Table I, we compare Christine 1D data to Eq. (20) [10]. The agreement is excellent for input power 30 dB below the input power that produces saturation at the output ($-30\,\mathrm{dB_{sat}}$). The agreement is less close for input powers of $-10\,\mathrm{dB_{sat}}$ and $0\,\mathrm{dB_{sat}}$ and this is probably due to the nonlinearities neglected in deriving the S-MUSE model [3]. In all cases, the agreement is very good (i.e., $<10\%$ error), indicating that the theory may be used for quantitative and qualitative studies of IMPs.

Next we consider a particular case with the drive frequency at the low end of the band such that the second and third harmonics are within the linear gain bandwidth. We consider the frequencies 1,2, and 3 GHz. In case 1, the drive frequency is $f_1=1$ GHz. In case 2, we also include $f_2=2$ GHz and $f_3=3$ GHz as drive frequencies as one might when using second- and third-harmonic injections.

In case 1, the frequency generation scheme (16) gives

$$\Omega^{(1)}=\{-f_1,f_1\}=\{-1,1\}, \tag{21}$$

$$\Omega^{(2)}=\{-2,2\}, \tag{22}$$

$$\Omega^{(3)}=\{-3,-1,1,3\}. \tag{23}$$

Formula (19) gives the growth rate of the 2 GHz term as

$$\mu_2^{(2)[1]}=\max\{2\mu_1^{(1)[1]},\nu_2^{[1]}\}=\nu_2^{[1]},$$

since the linear growth rate $\nu_2^{[1]}$ for 2 GHz is greater than two times the linear growth rate $\mu_1^{(1)[1]}=\nu_1^{[1]}$ for 1 GHz. Moreover, the growth rate for 3 GHz is

$$\mu_3^{(3)[1]}=\max\{\mu_1^{(1)[1]}+\mu_2^{(2)[1]},\nu_3^{[1]}\}=\mu_1^{(1)[1]}+\mu_2^{(2)[1]}.$$

That is, the growth rate for the third harmonic is the growth rate for the second harmonic plus the growth rate of the drive. Simulations of this case show that the second and third harmonics do not achieve their asymptotic growth rates prior to saturation. However, analytic solutions of Eq. (7) confirm that the growth rates predicted by Eq. (19) are those of the dominant terms.

In general application of Eq. (19), it is important to notice that the maximum growth rate $\mu_\ell^{(\alpha)[1]}$ is a function of α. A frequency f_ℓ may appear in several terms of the series, and each of these terms has a maximum growth rate $\mu_\ell^{(\alpha)[1]}$. In many cases, the observed growth rate in a simulation will be the maximum growth rate for the first term in the series for which the frequency appears, i.e., corresponding to the smallest α for which the frequency appears in $\Omega^{(\alpha)}$. For example, in case 1, Eqs. (21) and (23) show that $f_1=1$ GHz is in both $\Omega^{(1)}$ and $\Omega^{(3)}$ and the corresponding growth rates of these terms are $\mu_1^{(1)[1]}$ and $\mu_1^{(3)[1]}$. Although $\mu_1^{(3)[1]}>\mu_1^{(1)[1]}$, in simulations $\mu_1^{(3)[1]}$ is never observed and $\mu_1^{(1)[1]}$ characterizes the solution. However, a similar conclusion does not hold in case 2.

In case 2, the frequency generation scheme (16) gives

$$\Omega^{(1)}=\{-f_3,-f_2,-f_1,f_1,f_2,f_3\}=\{-3,-2,-1,1,2,3\},$$

$$\Omega^{(2)}=\{-6,-5,-4,-3,-2,-1,1,2,3,4,5,6\}.$$

Now $f_1=1$ GHz is in both $\Omega^{(1)}$ and $\Omega^{(2)}$. Since it is common for second-order products to reach the level of drive frequencies before the TWT saturates, in simulations we do see the $\alpha=2$ term for large enough drive levels of 2 GHz and 3 GHz. This phenomenon is shown in Fig. 1 for a Christine 1D simulation. Both the $\alpha=1$ and $\alpha=2$ maximum growth rates are observed and the $\alpha=2$ maximum growth rate is equal to the theoretically predicted sum of the growth rates driving it to within 1%.

By a mathematical treatment of an approximate nonlinear TWT model, we have yielded a new view of IMP generation and provided estimates for IMP growth rates. In this view, the generation of IMP frequencies is a sequential process wherein higher order IMPs are produced by combining lower order IMPs (and drive frequencies) via a quadratic nonlinearity. The quadratic nonlinearities are the velocity nonlinearity $v(\partial v/\partial z)$ in Newton's law and the definition of current ρv in the continuity equation [3]. We note that certain models of the klystron and free electron laser can be expressed in the same form (7) as S-MUSE, and therefore a similar method for understanding and predicting IMPs could be applied to these devices.

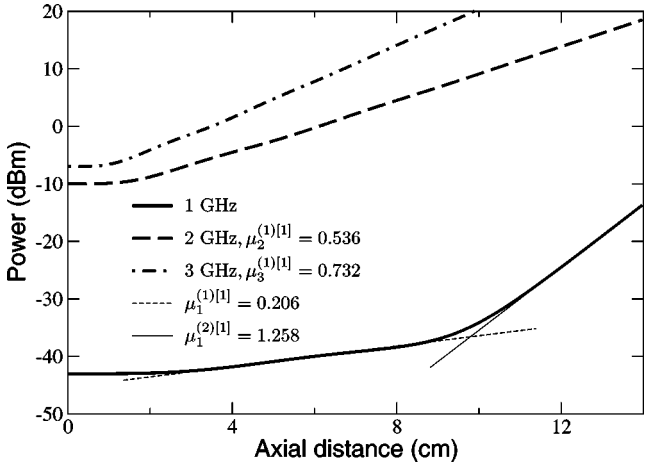

FIG. 1. Power versus axial distance for three harmonically related drive frequencies predicted by Christine 1D; 1 GHz is a second-order product of 2 GHz and 3 GHz and exhibits first its $\alpha=1$ maximum growth rate, then its $\alpha=2$ maximum growth rate produced by 2 GHz and 3 GHz.

Formula (19) indicates that the growth rate of an IMP is the greater of the sum of the growth rates of the frequencies combining to make the IMP and the linear growth rate of the IMP frequency. In most cases the former growth rate applies but there can be exceptions for very wide band TWTs. The analysis refines and gives insight into the conventional rule of thumb [2] of estimating the growth rate of a *K*th order IMP as *K* times the growth rate of the drive frequency.

J. G. Wöhlbier and J. H. Booske gratefully acknowledge support in part by the AFOSR Grant No. 49620-00-1-0088 and by the DUSD (S&T) under the Innovative Microwave Vacuum Electronics Multidisciplinary University Research Initiative (MURI) program, managed by the United States Air Force Office of Scientific Research under Grant No. F49620-99-1-0297.

[1] T.M. Antonsen, Jr., A. Mondelli, B. Levush, J.P. Verboncoeur, and C.K. Birdsall, Proc. IEEE **87**, 804 (1999).

[2] C. Armstrong (private communication).

[3] J.G. Wöhlbier, J.H. Booske, and I. Dobson, IEEE Trans. Plasma Sci. (to be published).

[4] R.G.E. Hutter, *Beam and Wave Electronics in Microwave Tubes* (Van Nostrand, Princeton, 1960).

[5] E.A. Coddington and N. Levinson, *Theory of Ordinary Differential Equations* (McGraw-Hill, New York, 1955), p. 78.

[6] M.A. Wirth, A. Singh, J.E. Scharer, and J.H. Booske, IEEE Trans. Electron Devices **49**, 1082 (2002).

[7] T.M. Antonsen, Jr. and B. Levush, IEEE Trans. Electron De-

vices **26**, 774 (1998).

[8] The series solution of Eq. (7) can be obtained by setting $\mathbf{x} = \boldsymbol{\epsilon}\mathbf{y}$, expanding in a power series in the parameter $\boldsymbol{\epsilon}$ and applying the method of small parameters; see e.g., S.G. Mikhlin and K.L. Smolitskiy, *Approximate Methods for Solution of Differential and Integral Equations* (American Elsevier, New York, 1967), p. 17.

[9] In general, $\mathbf{a}_\ell^{(\alpha)[p]}$ is a vector of polynomials in z, i.e., there are ''secular'' terms in the solution. We assume that $\mathbf{a}_\ell^{(\alpha)[1]}$ is a constant vector, i.e., the term containing the maximum growth rate never has a factor of z multiplying the complex exponential. The secular terms arise in the special case of exact ''resonance'' of eigenvalues of $\mathbf{A}_\ell$ for different values of ℓ. For example, to have a leading secular term in the harmonic solution, the dominant eigenvalue at the harmonic must be exactly equal to two times the dominant eigenvalue at the fundamental. For general dispersion, there is a zero probability of having such an eigenvalue resonance. However, in a dispersionless model secular terms must be accounted for and the present theory would need to be modified.

[10] Since we measure growth rates from power vs axial position data, we actually compare two times Eq. (20) to the data. However, we do not make this distinction in the text of the paper.